JOURNAL OF AIRCRAFT
Vol. 29, No. 4, July–Aug. 1992

Calibration-Related Pseudo-Reynolds Number Trends in Transonic Wind Tunnels

Felix Aulehla*
MBB-Deutsche Aerospace, Munich, Germany

Until the mid-seventies there were many variable density transonic wind tunnels which had been calibrated at only one total pressure. Today this still holds for some tunnels. If Reynolds number, i.e., total pressure, is varied in such tunnels during a test, small systematic errors in freestream Mach number M_0 do then result. In M_0-sensitive measurements this causes exaggerated (pseudo) Reynolds number trends. For the examples of afterbody pressure drag, transonic shock location, and transonic maximum lift, it is shown that up to 100% of these trends can be attributed to the lack of a full Reynolds number calibration. The remaining few percent must be due to true Reynolds number effects and to additional, yet unknown, systematic errors.

Nomenclature

AB = afterbody
C_{DAB} = afterbody drag coefficient referred to fuselage maximum cross section
C_{DPAB} = afterbody pressure drag coefficient referred to fuselage maximum cross section
C_{DPFB} = forebody pressure drag coefficient referred to fuselage maximum cross section
C_L = lift coefficient
C_P = pressure coefficient, $(P - P_0)/q_0$
C_{PW} = wall pressure coefficient
$\bar{C}_{PW}$ = mean value of all C_{PW} per run with Re and M_0 being constant
$\bar{\bar{C}}_{PW}$ = mean value of $\bar{C}_{PW}$ from all runs
FB = forebody
M_0 = freestream Mach number
M_W = wall Mach number, derived from mean wall pressures, $\approx M_{0\text{true}}$ (empty tunnel)
P_0 = freestream static pressure
P_P = plenum chamber pressure
P_{ref} = reference pressure, wall pressure located inside and upstream of test section
P_{TO} = freestream total pressure
P_W = test section wall pressure
$\bar{P}_W$ = mean value of all P_W per run with Re and M_0 being constant
q_0 = freestream dynamic pressure
R = radius of axisymmetric body
Re = Reynolds number, based on body length or wing mean chord
t/c = relative profile thickness
x/c = axial distance from leading edge referred to wing chord
x_s = shock location (at sonic conditions unless noted otherwise)
α = angle of incidence

I. Introduction

TRANSONIC Reynolds number effects have been a controversial subject over the past 20 yr. Discrepancies between wind-tunnel and flight test results often served as a convenient excuse to blame the inadequate simulation of the full-scale Reynolds number in subscale wind-tunnel testing for these discrepancies. One of the well-known examples of this is the transonic wing shock location of the Lockheed C-141 aircraft: in full-scale flight the wing shock location was about 20% chord further aft than in the subscale wind-tunnel test conducted at a much lower Reynolds number.[8,24]

The purpose of this article is to review such Reynolds number trends critically. This, of course, does not mean that the classical Reynolds number effects like friction, boundary-layer transition, low-speed separation on steep boattails, e.g., on the sphere, should be questioned. Also, any differences between wind tunnel and free flight which stem from wind-tunnel wall interference are not of concern here. For this subject the reader is referred to the standard wall interference correction methods as well as to the adaptive wind-tunnel wall technology.[16]

The present paper deals solely with the Reynolds number dependent changes of these wall interferences and with their influence on the data obtained from a model exposed to such varying boundary conditions at transonic speeds. It will be shown that these Reynolds number effects at the wind-tunnel wall are predominant and can completely mask the true effects on the model itself; that is, in Mach number-sensitive measurements the true Reynolds number effects are up to 100% smaller than quoted by many investigators. In a few cases these errors even exceed the value of 100% (sign reversal, "negative" Reynolds number trend). In the following sections, examples for such pseudo-Reynolds number trends will be given using measured and computed data on afterbody drag (Sec. III), maximum lift (Sec. IV), and transonic shock location (Sec. V).

It should be noted that Sec. II contains the discussion of the basic principles presented in the entire paper: in essence the errors in freestream Mach number and in the axial pressure gradient are identified as the main causes for the observed pseudo-Reynolds number effects. It will be explained why these errors always do occur in conventional variable density wind tunnels which have not been calibrated as a function of Reynolds number.

II. Incomplete Wind-Tunnel Calibration as Cause for Pseudo-Reynolds Number Effects

It appears trivial to request that an empty test section of a variable density wind tunnel be calibrated not only at all Mach numbers but also at all combinations of Mach and Reynolds numbers. Nevertheless, before 1975 many tunnels of this type

Presented as Paper 87-2612 at the AIAA 5th Applied Aerodynamics Conference, Monterey, CA, Aug. 17–19, 1987; received Aug. 12, 1990; revision received April 17, 1991; accepted for publication June 27, 1991.

*Chief Scientist, Flight Physics Department, Military Aircraft Division, P.O. Box 801160, 8000 Munich 80.

either did not have such a full Reynolds number calibration or did not use it.[7,23,30] Today there are still a few tunnels that ignore the importance of such a full Reynolds number calibration.

In calibrating the empty tunnel the mean value of the static pressure distribution inside the complete test section is often related to one single representative pressure which is then used in later testing to set the desired freestream Mach number. Normally this pressure is either the pressure in the surrounding plenum chamber or a wall pressure upstream of the test section (Fig. 1a).

In many transonic wind tunnels with ventilated test sections the calibration of the empty tunnel was performed essentially only at one, the nominal total pressure. For operations at different total pressures it was assumed that the ratio of the true static pressure relative to the reference pressure would not change significantly.[30] A rough check seemed to confirm this assumption; however, only after the author had introduced[2,3] the mean values of the (rather rugged[4]) wall pressure distributions, a clear, although small, deviation of the true freestream static pressure level from its nominal value became apparent and, hence, also the corresponding error in freestream Mach number. Depending on whether the reference pressure was inside or outside the test section, opposite trends a and b were found (Fig. 1b). In sensitive measurements like the measurement of afterbody pressure drag, transonic shock location, and transonic maximum lift these small deviations are of decisive importance, as will be explained later.

Fig. 2 shows a quantitative example of this unnoticed pressure level change measured 1974 in the 1 × 1 m Transonic Wind Tunnel Göttingen (TWG) of the German Aerospace Research Establishment (DLR, formerly DFVLR) before the

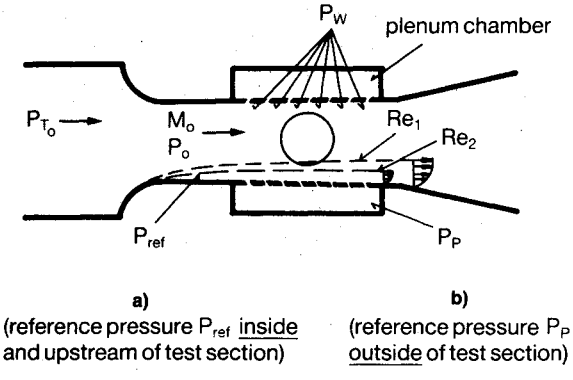

Fig. 1a Different reference pressures P_{ref} and P_P for setting the freestream Mach number M_0.[7]

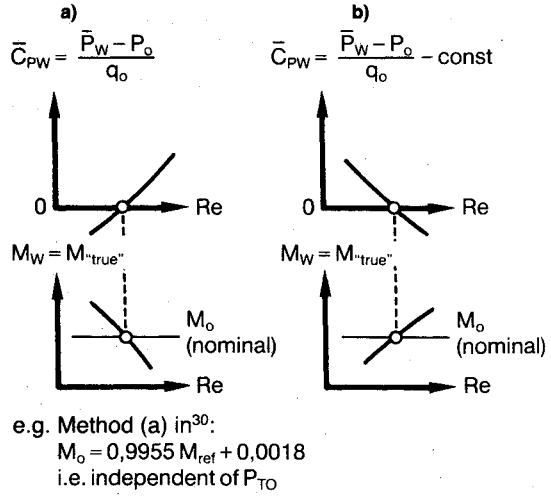

Fig. 1b Different reference pressures (P_{ref} and P_P) cause opposite trends in M_0 errors in wind tunnels without full Re calibration.[7]

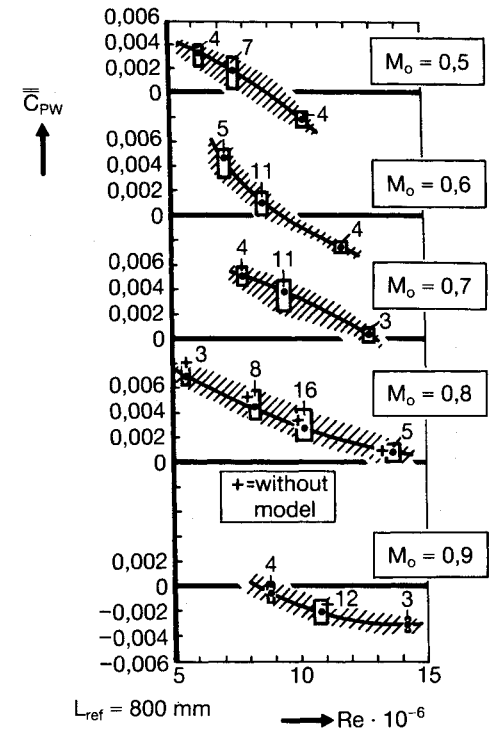

Fig. 2 Mean wall pressure coefficients in the TWG.[3]

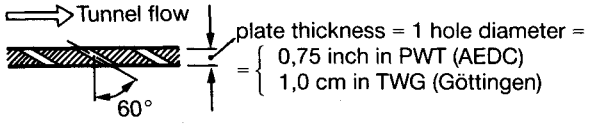

Fig. 3 Perforation of the four test section walls in the 16-ft PWT and the 1-m TWG.[4]

Reynolds number calibration was applied. In these measurements the pressure in the surrounding plenum chamber P_P was used as reference pressure to set the required Mach numbers (method b in Fig. 1). In Fig. 2 the wall pressures recorded during all runs of two test series (nos. 3 and 4) have been included. The pressure readings from all 24 pressure tappings along the centerline of the upper test section wall were averaged arithmetically for each individual run to give one value of $\bar{C}_{PW}$ per run. The numbers at each bar indicate how many runs at each Mach and Reynolds number were conducted (repeatability). Within each bar, these repeats were arithmetically averaged a second time to give $\bar{\bar{C}}_{PW}$ shown as dots and solid curves, respectively. The magnitude of the scatter is shown by the hatched band which is about 0.003 wide.

Comparing the cross symbols (empty tunnel) with the solid curve at $M_0 = 0.8$ it can be seen that the blockage of this model (1.13%) had little or no effect on the averaged wall pressures, i.e., on the pressure level in the test section. These test series 3 and 4 in the Göttigen tunnel were conducted in order to better understand the unexpected afterbody drag variation with Reynolds number measured in the 16-ft Arnold Engineering Development Center (AEDC) tunnel (see Sec. III). Since both tunnels had very similar test section wall geometries (Fig. 3) it was speculated by the author that the Reynolds number-dependent changes of the wall characteristics and hence the errors in freestream Mach number would also be similar. This assumption was later fully confirmed.

In Ref. 4 the following explanation for the change in wall-pressure coefficients with Reynolds number had been suggested. As the perforation of the four test-section walls consisted of circular holes inclined 60 deg from the vertical (Fig. 3) one can expect these holes to perform similarly as 30 deg flush boundary-layer inlets. When Reynolds number is raised

by increasing the tunnel total pressure, the wall boundary-layer becomes thinner, which results in an increase in pressure recovery through these inlets. That is, the plenum chamber pressure, which is used to set the freestream Mach number, goes up relative to the wall pressures. Without proper Reynolds number calibration this increase then feigns a too high wall pressure. Hence, the true wall pressure is lower, and the true freestream Mach number higher. So, instead of determining the desired Reynolds number influence on the model, one measures in reality primarily the influence of Mach number errors caused by the Reynolds number effects at the wind-tunnel wall.

To adjust the freestream Mach number some transonic wind tunnels do not use the plenum chamber pressure but a wall pressure inside and upstream of the test section (method a in Fig. 1). Reducing the tunnel Reynolds number causes the wall boundary-layer to grow in stream direction more rapidly. This increasing "nozzle effect" lowers the static pressure in the test section and raises the freestream Mach number relative to the upstream reference values.

A quantitative example of this second trend is shown in Fig. 4. The data were obtained from the 0.34 × 0.60 m Transonic Wind Tunnel of DLR Braunschweig (TWB) described in Ref. 30. Simple flat-plate boundary-layer calculations together with one-dimensional flow relations confirmed the trend in Fig. 4. As a further confirmation, the wall pressures in a similar tunnel, the 0.30 × 0.675 m transonic blowdown tunnel of the Universität der Bundeswehr München (TWM) were recorded in 1986 without applying the Reynolds number calibration. Details of this tunnel can be found in Ref. 31. The mean wall pressure coefficients showed practically the same variation with Reynolds number as those from the TWB, see, e.g., Fig. 6 in Ref. 8 or Fig. 2.17 in Ref. 9.

So far, only (unnoticed) changes in the pressure level, i.e., errors in the freestream Mach number, have been discussed. These can be avoided by a full Reynolds number calibration of the empty tunnel, which means calibration at all density and Mach number combinations. However, in addition to

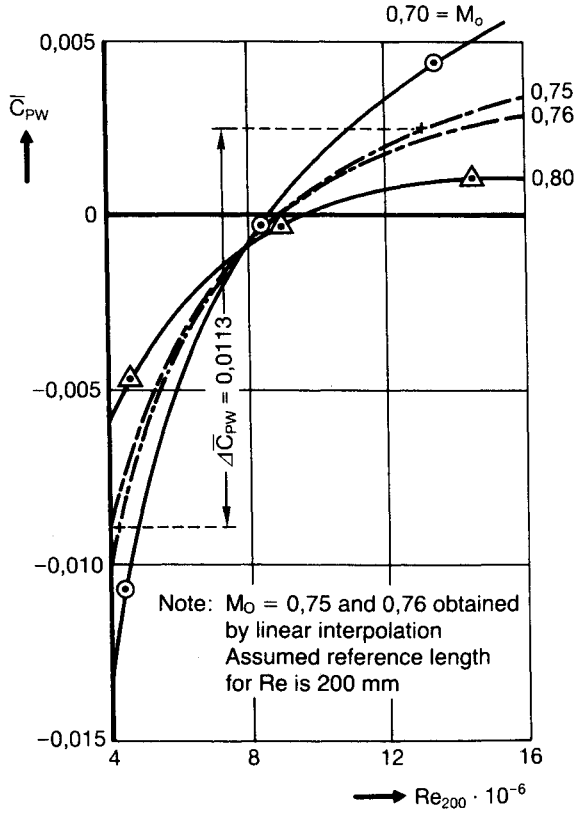

Fig. 4 Mean wall pressure coefficients in the empty test section of the TWB, derived from data in Ref. 21.

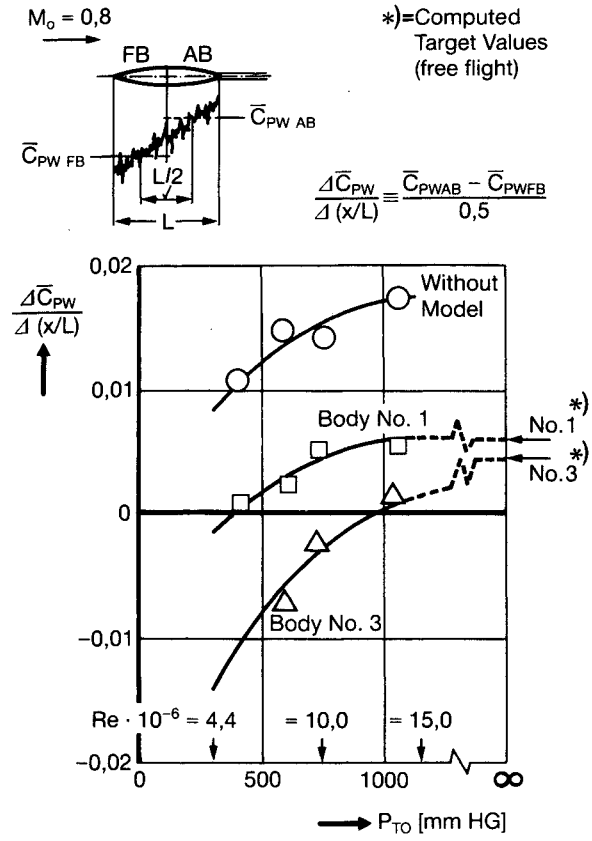

Fig. 5 Effect of tunnel total pressure on measured pressure gradient at upper test section wall in the TWG.[4]

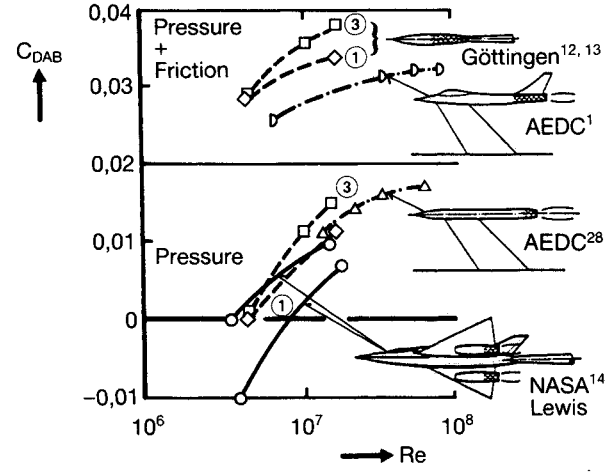

Fig. 6 Reynolds number effect on afterbody drag obtained from different wind tunnels.[2]

these Mach number errors, there are also changes in the axial pressure gradient produced by the varying rate of growth of the wind-tunnel wall boundary layer.

Figure 5 shows these (linearized) gradients measured by the 24 wall-pressure tappings in the TWG. Since both test-section side-walls were kept divergent at a constant angle of 0.5 deg relative to the tunnel centerline, the upper curve for the empty test section indicates a positive pressure gradient, which becomes even more positive as Reynolds number is raised, i.e., as the wall boundary layer gets thinner (increased diffuser effect). The presence of the models reduces this diffusion effect. However, the trend with Reynolds number for all three curves is roughly the same. This means that during a Reynolds number variation the changes in axial pressure gradient of the overall flowfield in the test section are primarily caused by the changes of the wall boundary layer rather than by those of the model boundary layer. To avoid also this

type of falsifying conditions requires changing the test section wall divergence angle during a variation of tunnel Reynolds number (density). This, however, normally is not done in conventional, i.e., in nonadaptive test sections.

As a consequence, such measurements need correcting by computations. Examples have been given in Ref. 5 for the transonic shock travel on an axisymmetric fuselage and on a Whitcomb-profile. For typical combinations of errors in Mach number and in axial pressure gradient as measured in the TWG before its full Reynolds number calibration, the computed corrections in shock travel due to incorrect axial pressure gradient were considerably smaller than those due to the error in Mach number, that is less than one third.[5] This ratio appears to be even smaller for the TWB. For this reason and also because of the lack of computed corrections in maximum lift and afterbody flow separation, the errors due to incorrect axial pressure gradient will not be discussed in this paper.

III. Afterbody Pressure Drag

Several wind tunnel investigations conducted in the early seventies showed an increasing trend of the afterbody pressure drag coefficient with Reynolds number (Fig. 6). However, a constant or even slightly decreasing trend similar to that of the turbulent flat plate friction coefficient had been expected. Therefore, the late Prof. Antonio Ferri from the New York University initiated in May 1972 the AGARD research project on "Improved Nozzle Testing Techniques in Transonic Flow."

First results were presented 1974 in Rome, where the contribution from Messerschmitt-Bölkow-Blohm GmbH (MBB)

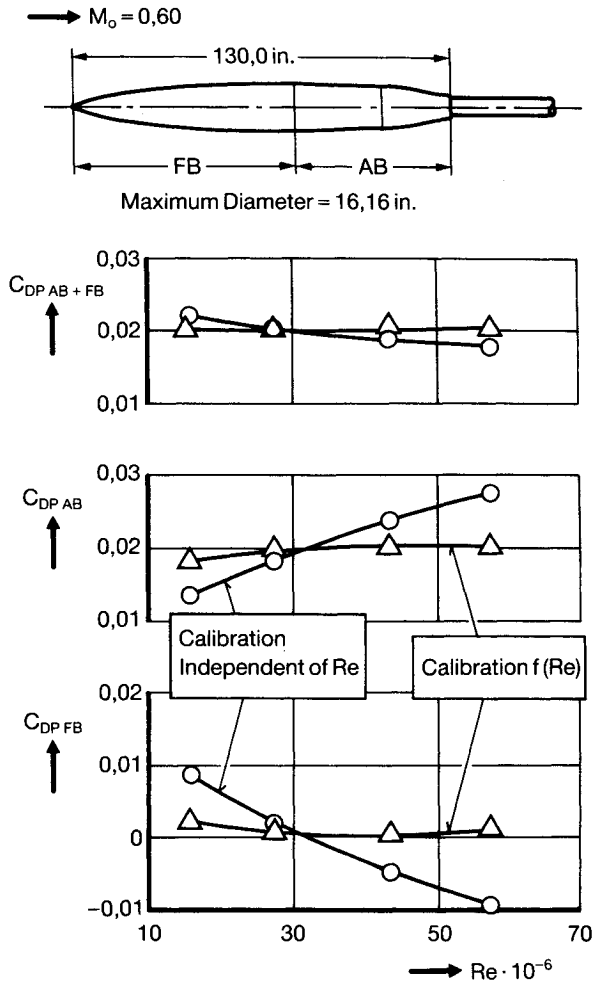

Fig. 7 Effect of wind-tunnel calibration on fore- and afterbody pressure drag coefficient.[29]

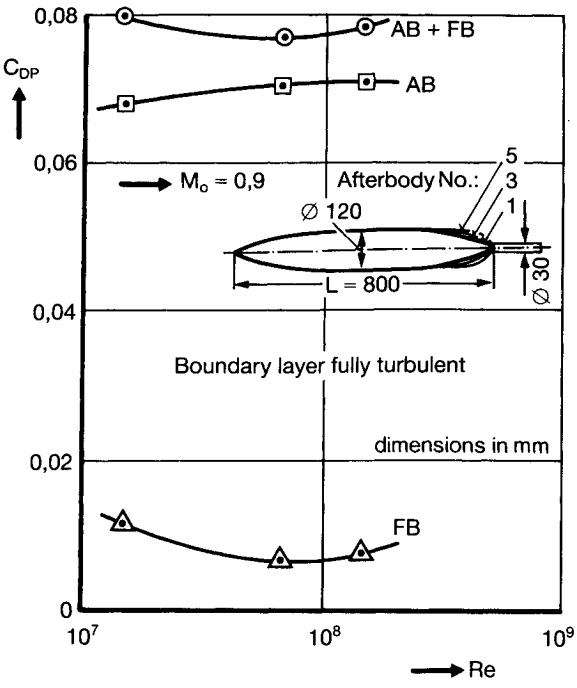

Fig. 8 Computed Reynolds number effect on fore- and afterbody pressure drag coefficient for MBB-body No. 5.[18]

showed[2] that this increasing trend in afterbody pressure drag coefficient measured in variable density wind tunnels was caused by a systematic error in freestream static pressure. It was also shown that, as a consequence, this trend was virtually completely compensated by the corresponding decrease in forebody pressure drag coefficient.

Proof for this systematic error had been given by the behavior of the mean wall pressure coefficients in the test section: instead of staying constant during a Reynolds number (total pressure) variation, they changed in the same sense and by the same amount as those on the model.[2] Removing the model neither changed the absolute values of the mean wall pressure coefficients nor their variation with Reynolds number (Fig. 2). Hence it was clear that the missing Reynolds number calibration of this tunnel was responsible for the systematic error in the static pressure level. The final results of the AGARD research project were published[3] in October 1975 and corroborated the early findings on Reynolds number effects in Ref. 2.

Above results were also confirmed by AEDC. After their 16-ft Propulsion Wind Tunnel had received a full Reynolds number calibration[23] in response to the findings in Ref. 2, they could show that afterbody and forebody pressure drag coefficients were (apart from local effects) no longer dependent on Reynolds number in the range investigated (Fig. 7). It is most interesting that this result applies not only to attached but also to separated flows on curved boattail contours, as will be shown below.

An independent Navier-Stokes computation by Deiwert[18] on the MBB-body No. 5 in the Reynolds number range from 14.5 to 145 Mio showed very little effect of Reynolds number on afterbody and forebody pressure drag coefficients (Fig. 8). The boundary layer was assumed to be fully turbulent.

A similar result was obtained by Reubush and Putnam in the Langley ½-m cryogenic tunnel.[27] They tested four afterbody contours with two forebodies of different lengths at Mach numbers 0.6 and 0.9 and Reynolds numbers from 2.5 Mio up to 130 Mio. The Reynolds number variation was achieved by changing the tunnel total pressure from 1.2 to 5.0 atmospheres and the stagnation temperature from 103 to 308 K. Boundary-layer transition was not fixed. Apart from the well-known, mutually compensating local effects, i.e., in-

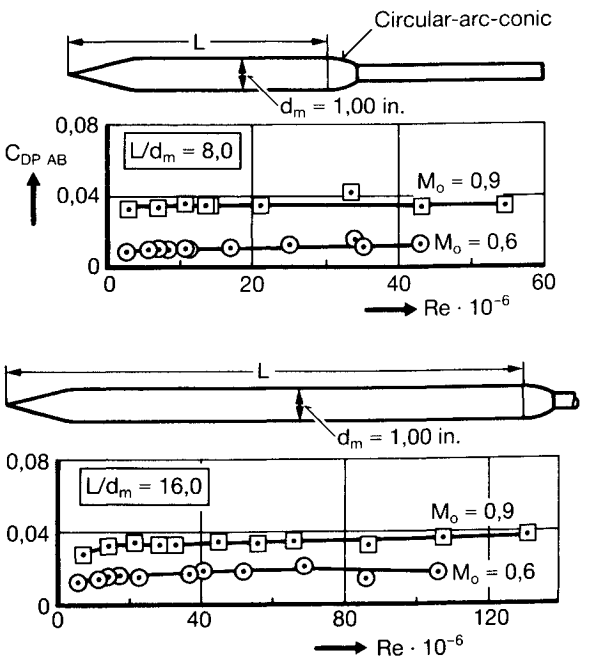

Fig. 9 Effect of Reynolds number on boattail pressure drag coefficient of circular-arc-conic boattails.[27]

creased expansion and recompression on the afterbody with increasing Reynolds number, practically no Reynolds number effects on afterbody pressure drag coefficient could be detected (Fig. 9). This result is most remarkable in that it applies to a very large Reynolds number range and in addition also covers, in contrast to the above computation by Deiwert, the low Reynolds number end.

In summary, the pressure drag coefficient of the afterbody (and forebody) seems to depend on Reynolds number by orders of magnitudes less than had been reported from many experiments. This immediately raises the heretical question of whether the transonic maximum lift coefficient of profiles and wings with fixed boundary-layer transition is also independent on Reynolds number in the range considered.

IV. Transonic Maximum Lift

Pressure plotting tests were conducted by DLR in their TWB on the supercritical profile type CAST 7/DoA1 using two models with 150- and 200-mm chord lengths.[25] The boundary-layer transition was fixed at 7% chord on upper and lower sides of the profile. The increase in maximum lift coefficient due to raising the Reynolds number from 6 to 11 Mio is shown in Fig. 10. The marked reduction in transonic maximum lift coefficient with increasing Mach number is illustrated in Fig. 11. The slopes at $M_0 = 0.70$ and 0.76 have been graphically determined in this figure to assess the sensitivity of $C_{L\max}$ against M_0-errors. Simple one-dimensional flow functions were used to compute the sensitivity of the freestream Mach number to errors in freestream static pressure ($=P_W$) in Table 1.

In Fig. 4 it was shown that the mean wall pressure coefficients in the TWB increased with Reynolds number which corresponds to a decrease of the true Mach number relative to its nominal value. The corresponding increase in maximum lift coefficient is then obtained using the slopes from Fig. 11. The following equations apply:

$$\Delta C_{L\max} = \underbrace{\frac{\Delta C_{L\max}}{\Delta M_0}}_{\text{from Fig. 11}} \cdot \underbrace{\left|\frac{\Delta M_0/M_0}{\Delta \bar{C}_{PW}}\right|}_{\text{from Table 1}} \cdot \underbrace{M_0 \cdot \Delta \bar{C}_{PW}}_{\text{from Fig. 4}} \qquad (1)$$

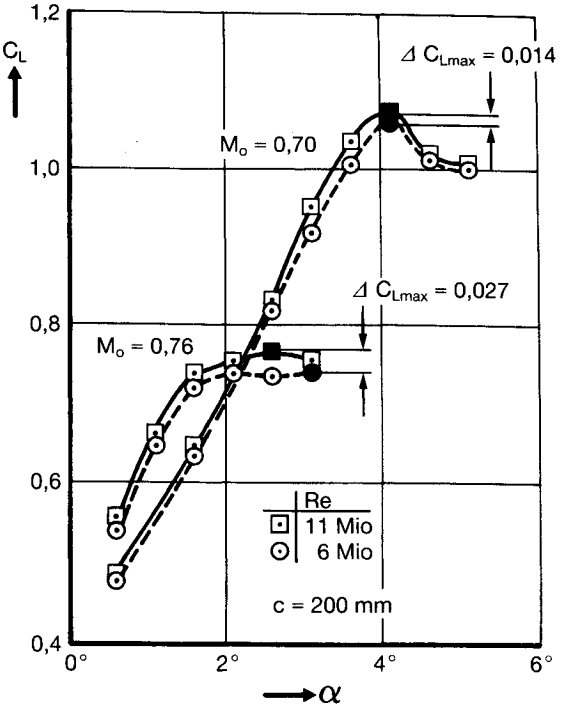

Fig. 10 Increase in maximum lift coefficient due to increasing Reynolds number from 6 to 11 Mio, CAST 7/DoA1.[25]

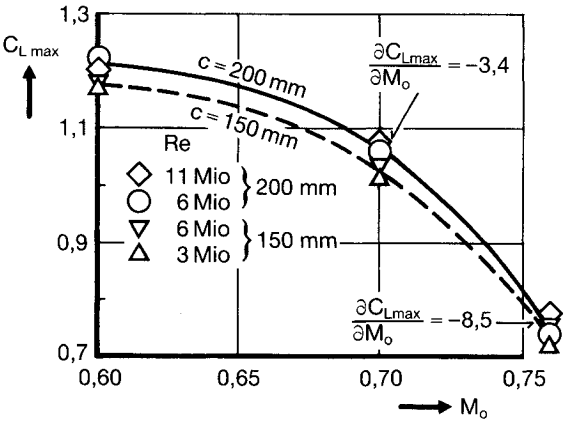

Fig. 11 Decrease of maximum lift coefficient with Mach number, derived from data in Ref. 25.

Table 1 Dependence of the relative Mach number error $\Delta M_0/M_0$ on the change in mean wall pressure coefficient $\Delta \bar{C}_{PW}$ (change in true freestream pressure)[3]

M_0 =	0.70	0.75	0.76	0.80
$\frac{\Delta M_0/M_0}{\Delta \bar{C}_{PW}}$ =	−0.549	−0.556	−0.558	−0.564

For $M_0 = 0.76$ Eq. (1) becomes

$$\Delta C_{L\max} = (-8.5)(-0.558)0.76\Delta \bar{C}_{PW} = 3.605\Delta \bar{C}_{PW} \qquad (2)$$

Using Eq. (2) the error in lift coefficient was computed in Table 2 for the change in mean wall pressure coefficient of Fig. 4. However, to obtain these $\bar{C}_{PW}$ for the 150 mm profile its Reynolds number had to be converted to the nominal reference length (200 mm) used in the empty tunnel tests, see line 4 in Table 2.

Analogous tables for the lower Mach number and for the larger profile can be found in Ref. 7. The "success rate,"

Table 2 Measured and computed changes in maximum lift coefficient for the profile with 150-mm chord length at $M_o = 0.760$

(1)	Re_{150} =	3.11 Mio	6.12 Mio		Result
(2)	$(C_{L\max})$ =	0.717	0.750	→	$(\Delta C_{L\max})_M$ = 0.033 (measured)
(3)	α =	3.10 deg	2.60 deg		
(4)	(200/150) Re_{150} = Re_{200} =	4.15 Mio	8.16 Mio	→	$\bar{C}_{PW}$ (from Fig. 4)
(5)	$\bar{C}_{PW}$ =	−0.0085	−0.0008	→	$\Delta\bar{C}_{PW}$ = 0.0077
(6)	Eq. (2) ≡	$(\Delta C_{L\max})_C = 3.605 \cdot \Delta\bar{C}_{PW}$		=	0.0278 (computed)
(7)	"Success rate" ≡	$(\ )_C/(\ )_M$		=	**84.1%** (computed/measured)

Table 3 Ratio of computed to measured change in maximum lift coefficient for the profile type CAST 7/DoA1

Chord length =	150 mm	200 mm
Increase in Re =	(3 → 6) Mio	(6 → 11) Mio
M_o = 0.70	98%[a]	72%
M_o = 0.76	84%	62%
Mean value =	**79%**	

[a]Extrapolation to Re_{200} = 3.77 Mio was required to obtain $\bar{C}_{PW}$ from Fig. 4.

which is the ratio of computed to measured change in transonic maximum lift coefficient

$$(\Delta C_{L\max})_C/(\Delta C_{L\max})_M$$

was supplemented from these tables and is summarized in Table 3.

Table 3 shows that an average of 79% of the increase in maximum lift coefficient measured in the TWB was in fact caused by calibration related errors in freestream Mach number. The remaining 21% are due to true Reynolds number effects on one hand and further (yet unknown) measuring errors on the other hand.

One of these, for example, could be the test section boundary-layer displacement thickness which modifies the flowfield of the model differently depending on whether a thin or thick initial wall boundary layer was present. An experimental investigation to eliminate these Reynolds number-dependent changes in wall disturbance by the provision of displacement bodies at the wind-tunnel wall was suggested in Ref. 6.

A further source of pseudo-Reynolds number effects is the freesteam flow angularity which changes with tunnel Reynolds number.[10] There are, of course, many more—not necessarily calibration-related—pseudo-Reynolds number effects, as Binion has summarized concisely in Ref. 19. A rather comprehensive description of observed Reynolds number effects and present boundary-layer simulation techniques was compiled in Ref. 15.

V. Transonic Shock Location

Shock movement due to Reynolds number changes measured in variable density wind tunnels was in the past completely attributed to Reynolds number effects on the model itself. It will be shown in the following that this behavior is in reality again almost entirely the result of Reynolds number-dependent changes of the test section wall interferences.

The experimental data, i.e., both the shock travel and the wall pressures, were obtained from the TWB of DLR Braunschweig. The wind tunnel is described in Ref. 30. The model tested was the supercritical profile Korn No. 1. The chord length was 127 mm, the relative thickness 11.7%. The theoretical geometry is defined in Ref. 11 and Ref. 20. Further model details, including the manufacturing deviations, are described in Ref. 20. There were no boundary-layer transition fixing devices such as roughness strips used. However, the experimenters from DLR Braunschweig claimed that the concentration of the pressure plotting holes at midspan resulted in an effectively fixed transition.[26]

The shock location has been defined here to be at C_P = −0.8, that is at the middle of the pressure "jump" and is

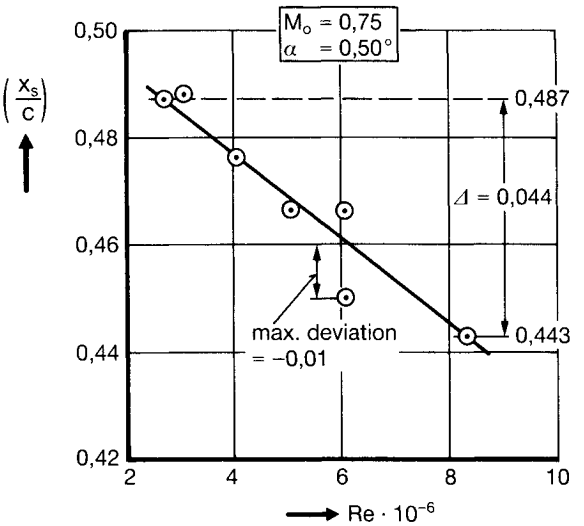

Fig. 12 Shock travel vs Reynolds number on Korn No. 1 airfoil measured in the TWB, derived from data in Ref. 22.

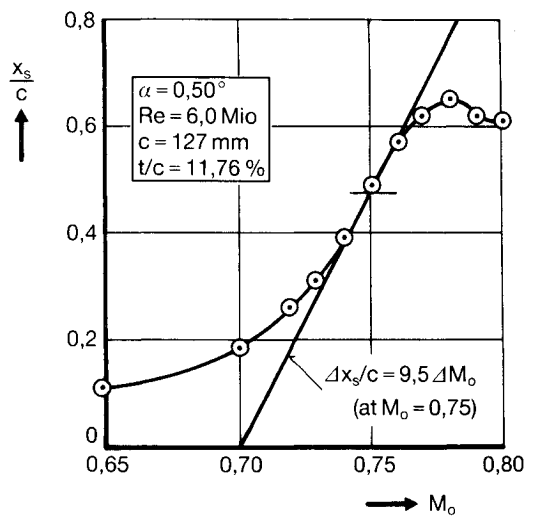

Fig. 13 Shock travel vs freestream Mach number M_0 on Korn No. 1 airfoil, derived from data in Ref. 20.

plotted vs Reynolds number in Fig. 12. Raising the Reynolds number from 2.70 to 8.31 Mio causes the shock to move forward by Δx_s = 4.4% c. Since increasing the Reynolds number normally moves the shock backwards, the present shock travel was sometimes referred to as "negative" Reynolds number effect. Keeping all variables except M_0 constant, results in the expected shock travel vs M_0, i.e., the shock moves rearwards with increasing M_0 (Fig. 13). At M_0 = 0.75 the slope of this curve gives a sensitivity against M_0-errors of $\Delta x_s/c$ = 9.5 ΔM_0.

Since above Reynolds numbers are referred to the profile chord length of 127 mm, while the wall pressures of the empty tunnel are plotted against a Reynolds number having a nominal reference length of 200 mm, the profile Reynolds num-

bers were multiplied by 200/127. This results in a Reynolds number range of 4.25–13.09 Mio. According to Fig. 4 this Reynolds number change corresponds in the TWB to an increase of the mean wall pressure coefficient by $\Delta\bar{C}_{PW} = 0.0113$. From Table 1 the sensitivity of the relative M_0 error against a change in the mean wall pressure coefficient at $M_0 = 0.75$ is obtained as

$$\Delta M_0/M_0 = -0.556 \cdot \Delta\bar{C}_{PW}$$

With above change in the mean wall pressure coefficients the M_0 error is then determined as

$$\Delta M_0 = -0.556 \cdot 0.0113 \cdot 0.750 = -0.00471$$

The negative sign indicates that the true M_0 decreases with increasing Reynolds number. Using the sensitivity of the shock location from Fig. 13, the forward movement of the shock is then obtained to be

$$\Delta(x_s/c) = \Delta M_0 \cdot \left(\frac{\Delta x_s/c}{\Delta M_0}\right)$$

$$= -0.00471 \cdot (9.5) = -0.0448 \approx -4.5\%$$

That is, solely due to this error in M_0 the shock must move forward by 4.5%. This is 0.1% c more than the measured value in Fig. 12. This means that in a flow free of M_0 errors the shock moves by no means forward but minimally (0.1% c) rearwards for the Reynolds number range considered.

In summary, the negative Reynolds number effects, that is the forward movement of the shock with increasing Reynolds number measured in the TWB, can be completely explained by the errors in freestream Mach number (fixed boundary-layer transition). Such errors are inherent in all empty tunnel calibrations which ignore variations in Reynolds number, i.e., in tunnel density.

In the present example, the sensitivity of the shock location towards errors in freestream Mach number was $\Delta x_s/c = 9.5\ \Delta M_0$ at $M_0 = 0.75$ and $\alpha = 0.50$ deg. The same reference shows an increased sensitivity of $\Delta x_s/c = 14.8\ \Delta M_0$ at a reduced incidence of 0.25 deg. Unfortunately no Reynolds number variation was tested at this incidence. A 56% greater spurious Reynolds number effect would then have been found. Similarly, had this model been tested in a wind tunnel in which the wall pressure coefficients decrease with increasing Reynolds number, like, for example, in the Göttingen or the 16-ft AEDC transonic tunnels prior to their full Reynolds number calibration, then the shock would not have moved forward by 4.4% c but backwards by a similar amount. No attempt was made to conduct a profound error analysis; however, some considerations on accuracy can be found in Refs. 7 and 9.

VI. Conclusions and Recommendations

1) Until the mid-seventies there were many variable density wind tunnels which were not calibrated over their full Reynolds number range but only at one, the nominal freestream total pressure. Today there are still some wind tunnels which ignore the importance of such a full Reynolds number calibration for sensitive measurements. This calibration defect causes errors primarily in the freestream Mach number and in the axial pressure gradient, which results in the discussed spurious Reynolds number effects.

2) Depending on whether the reference pressure tapping used to set the freestream Mach number is located outside or inside the test section of such tunnels, positive or negative pseudo Reynolds number effects do then result.

3) The mean value of the wall pressures in the empty test section is an excellent means of detecting even very small errors in freestream Mach number and changes in axial pressure gradient during a Reynolds number variation while all other parameters including wall porosity and wall divergence are kept constant.

4) The true transonic Reynolds number effects are up to 100% smaller than quoted from sensitive experiments in wind tunnels without full Reynolds number calibration. Sensitive are all measurements the results of which change markedly with freestream Mach number (and/or with axial pressure gradient and incidence). Examples have been given for the afterbody pressure drag, the transonic maximum lift, and the transonic shock location. The same should hold for other transonic effects like buffet, drag rise, etc. It is suggested that all transonic Reynolds number effects of larger amount be questioned unless the experimenters clearly specify when and with what accuracy their tunnel had been calibrated over its full Reynolds number range.

5) For all variable density wind tunnels without full Reynolds number calibration it is recommended to measure as a first step the wall pressures at all densities in order to supplement the existing empty tunnel calibration. This not only helps future tests but would also permit correction of previous results.

Acknowledgments

The author gratefully acknowledges the cooperation of the German research groups of DLR. In particular, mention should be made of Wolfgang Lorenz-Meyer, previously with DLR Göttingen, who provided in the early seventies, the wall pressures for the positive Reynolds number effects while Heinz Hoheisel of DLR Braunschweig supplied the corresponding data including the transonic shock travel for the "negative" Reynolds number effects from the Braunschweig tunnel.

Thanks are also due to AEDC who confirmed the findings from the Göttingen measurements in their 16-ft transonic tunnel while Siegfried Wagner at the University of the Bundeswehr in Munich corroborated the evidence from Braunschweig in his tunnel. Lastly, the author wishes to thank his colleague Geert Besigk for his valuable assistance throughout the entire effort, Ted Carter, formerly with ARA Bedford, for his advice at the beginning of this work, and the late Antonio Ferri, in particular, who initiated this research project in May 1972.

References

[1]Antonatos, P. P., Surber, L. E., Laughrey, J. A., and Stava, D. J., "Assessment of the Influence of Inlet and Aftbody/Nozzle Performance on Total Aircraft Drag," AGARD-CP-124-15, April 1973.

[2]Aulehla, F., and Besigk, G., "Reynolds Number Effects on Fore- and Aftbody Pressure Drag," AGARD-CP-150-12, Sept. 1974.

[3]Aulehla, F., and Besigk, G., "Fore- and Aftbody Flow Field Interaction with Consideration of Reynolds Number Effects," Agard-AG-208-II-F, Oct. 1975.

[4]Aulehla, F., "Drag Measurement in Transonic Wind Tunnels," AGARD-CP-242-7, Oct. 1977.

[5]Aulehla, F., and Eberle, A., "Reynolds Number Effects on Transonic Shock Location," AGARD-CP-335-4, May 1982.

[6]Aulehla, F., "Re-Zahleinfluß auf Windkanal-Wandinterferenz und auf C_{Amax}," Meeting Minutes, MBB FE124-BP-013-18.1.84, Jan. 1984.

[7]Aulehla, F., "Pseudo Reynolds Number Trends," MBB Rept. LKE 124-S-R-1584, Dec. 1986.

[8]Aulehla, F., "Pseudo Reynolds Number Trends," AIAA Paper 87-2612, Aug. 1987.

[9]Aulehla, F., "Pseudo-Reynoldszahleffekte in transsonischen Windkanälen," Dissertation at Rheinisch-Westfälische Technische Hochschule Aachen, Aug. 1989.

[10]Aulehla, F., "Reynolds Number Dependent Flow Angularity in Transonic Wind Tunnels," MBB FE21-S-TN-257, March 1991.

[11]Bauer, F., Garabedian, P., Korn, D., and Jameson, A., "Supercritical Wing Sections II," *Lecture Notes in Economics and Mathematical Systems*, Springer-Verlag, New York, 1975.

[12]Besigk, G., "Halbempirische Theorie zur Bestimmung des Heckwiderstandes," MBB Rept. UFE 628/1-70, March 1971.

[13]Besigk, G., "Reynoldszahleffekte bei der Widerstandsbestim-

mung," MBB Rept. UFE 1078, Jan. 1974.
[14]Chamberlin, R., and Blaha, B. J., "Flight and Wind Tunnel Investigation of the Effects of Reynolds Number on Installed Boattail Drag at Subsonic Speeds," AIAA Paper 73-139, Jan. 1973 (see also Wilcox and Chamberlin, AGARD-CP-150-21, Sept. 1974).
[15]Chan, Y. Y., Michel, R., et al. "Boundary Layer Simulation and Control in Wind Tunnels" (WG 09), AGARD-AR-224, April 1988.
[16]Chevallier, J. P., Ciray, C., et al., "Adaptive Wind Tunnel Walls: Technology & Applications" (WG 12), AGARD-AR-269, April 1990.
[17]Data from Testing Five Bodies of Revolution in the Göttingen Transonic Wind Tunnel, 1970/1972/1974, unpublished except for body No. 3: "Experimental Data Base for Computer Program Assessment" (WG04), AGARD-AR-138-C2, May 1979.
[18]Deiwert, G. S., "Computed Pressure Distribution on Axisymmetric MBB Body No. 5 at $M = 0.9$," NASA Ames, Personal communication, March 15, 1982.
[19]Elsenaar, A., Binion, T. W., Jr., Stanewsky, E., and Hornung, H. G., "Reynolds Number Effects in Transonic Flow," AGARD-AG-303, Dec. 1988.
[20]Heinrichs, W., "Messungen am Profil Korn No. 1 im Transsonischen Windkanal der DFVLR in Braunschweig (TWB)," DFVLR IB 129-81/20, Nov. 1981.
[21]Hoheisel, H., Personal communication on the Wall Pressures in the Transonic Wind Tunnel Braunschweig, Ho/Mei/129, March 30, 1982.
[22]Hoheisel, H., Personal communication, Test Results from Korn Profile No. 1 in the Transonic Wind Tunnel Braunschweig, Ho/Mei/129, May 11, 1982.
[23]Jackson, F. M., "Calibration of the AEDC-PWT 16ft Transonic Tunnel with the Propulsion Test Section at Various Reynolds Numbers," AEDC TR-77-121, Report Date: Aug. 1978, Reporting Period: Oct. 1974–June 1975.
[24]Loving, D. L., "Wind-Tunnel-Flight Correlation of Shock-Induced Separated Flow," NASA TN D-3580, Sept. 1966.
[25]Puffert-Meißner, W., "Data Report on the Cast 7/DoA1 Airfoil in the Transonic Wind Tunnel Braunschweig," DFVLR IB 129-82/2, March 1982, Contribution for GARTEUR Group 02 on "Two-dimensional Transonic Testing Methods."
[26]Puffert-Meißner, W., Personal communication on Boundary Layer Transition and Shock Location, Nov. 29, 1990.
[27]Reubush, D. E., and Putnam, L. E., "An Experimental and Analytical Investigation of the Effect on Isolated Boattail Drag of Varying Reynolds Number up to 130×10^6," NASA TN D-8210, May 1976.
[28]Richey, G. K., Preliminary Data of the AGARD Ad Hoc Study "Improved Nozzle Testing Techniques in Transonic Flow," AFFDL, March 1974.
[29]Spratley, A. V., Thompson, E. R., and Kennedy, T. L., "Reynolds Number and Nozzle Afterbody Configuration Effects on Model Forebody and Afterbody Drag," AIAA Paper 77-103, Jan. 1977.
[30]Stanewsky, E., Puffert-Meißner, W., Müller, R., and Hoheisel, H., "Der Transsonische Windkanal Braunschweig der DFVLR," DFVLR IB 129-82/1, Feb. 1982, also in ZFW 6, 1982, pp. 398–408.
[31]Wagner, S., and Hampel, A., "Der Transsonische Windkanal des Instituts fur Luftfahrttechnik und Leichtbau der HSBw München," Jahrestagung der DGLR, Hamburg, Oct. 1984.